# Compact electric-*LC* resonators for metamaterials

**Withawat Withayachumnankul**[1,2], **Christophe Fumeaux**[1], **and Derek Abbott**[1]

[1]*School of Electrical & Electronic Engineering, University of Adelaide, SA 5005, Australia*

[2]*School of Electronic Engineering, Faculty of Engineering*
*King Mongkut's Institute of Technology Ladkrabang, Bangkok 10520, Thailand*
withawat@eleceng.adelaide.edu.au

**Abstract:** Alternative designs to an electric-*LC* (ELC) resonator, which is a type of metamaterial inclusion, are presented in this article. Fitting the resonator with an interdigital capacitor (IDC) helps to increase the total capacitance of the structure. In effect, its resonance frequency is shifted downwards. This implies a decreased overall resonator size with respect to its operating wavelength. As a result, the metamaterial, composed of an array of IDC-loaded ELC resonators with their collective electromagnetic response, possesses improved homogeneity and hence is less influenced by diffraction effects of individual cells. The impact of incorporating an IDC into ELC resonators in terms of the electrical size at resonance and other relevant properties are investigated through both simulation and experiment in the microwave regime. The proposed structures can be applied to the terahertz regime via appropriate lithographic scaling.



**OCIS codes:** (160.1245) Artificially engineered materials; (160.3918) Metamaterials; (260.2065) Effective medium theory; (350.4010) Microwaves

## References and links

1. J. B. Pendry, A. J. Holden, D. J. Robbins, and W. J. Stewart, "Magnetism from conductors and enhanced nonlinear phenomena," IEEE Trans. Microwave Theory Tech **47**, 2075–2084 (1999).
2. V. Shalaev, W. Cai, U. Chettiar, H. Yuan, A. Sarychev, V. Drachev, and A. Kildishev, "Negative index of refraction in optical metamaterials," Opt. Lett. **30**, 3356–3358 (2005).
3. J. B. Pendry, "Negative refraction makes a perfect lens," Phys. Rev. Lett. **85**, 3966–3969 (2000).
4. N. Fang, H. Lee, C. Sun, and X. Zhang, "Sub-diffraction-limited optical imaging with a silver superlens," Science **308**, 534–537 (2005).
5. D. Schurig, J. J. Mock, B. J. Justice, S. A. Cummer, J. B. Pendry, A. F. Starr, and D. R. Smith, "Metamaterial electromagnetic cloak at microwave frequencies," Science **314**, 977–980 (2006).
6. N. A. Zharova, I. V. Shadrivov, A. A. Zharov, and Y. Kivshar, "Ideal and nonideal invisibility cloaks," Opt. Express **16**, 21369–21374 (2008).
7. T. Koschny, P. Markoš, E. N. Economou, D. R. Smith, D. C. Vier, and C. M. Soukoulis, "Impact of inherent periodic structure on effective medium description of left-handed and related metamaterials," Phys. Rev. B: Condens. Matter **71**, art. no. 245105 (2005).
8. C. Caloz, A. Lai, and T. Itoh, "The challenge of homogenization in metamaterials," New J. Phys. **7**, art. no. 167 (2005).
9. D. R. Smith, D. Schurig, M. Rosenbluth, S. Schultz, S. A. Ramakrishna, and J. B. Pendry, "Limitations on subdiffraction imaging with a negative refractive index slab," Appl. Phys. Lett. **82**, 1506–1508 (2003).
10. M. M. Lapine and S. Tretyakov, "Contemporary notes on metamaterials," IET Microwaves Antennas Propag. **1**, 3–11 (2007).

#135576 - $15.00 USD Received 23 Sep 2010; revised 3 Nov 2010; accepted 23 Nov 2010; published 26 Nov 2010

11. D. Rialet, A. Sharaiha, A.-C. Tarot, and C. Delaveaud, "Characterization of antennas on dielectric and magnetic substrates effective medium approximation," in "Third European Conference on Antennas and Propagation (EuCAP)," (2009), pp. 3163–3166.
12. K. Aydin, I. Bulu, K. Guven, M. Kafesaki, C. M. Soukoulis, and E. Ozbay, "Investigation of magnetic resonances for different split-ring resonator parameters and designs," New J. Phys. **7**, art. no. 168 (2005).
13. K. Aydin and E. Ozbay, "Capacitor-loaded split ring resonators as tunable metamaterial components," J. Appl. Phys. **101**, 024911 (2007).
14. F. Bilotti, A. Toscano, and L. Vegni, "Design of spiral and multiple split-ring resonators for the realization of miniaturized metamaterial samples," IEEE Trans. Antennas Propag. **55**, 2258–2267 (2007).
15. J. D. Baena, R. Marqués, and F. Medina, "Artificial magnetic metamaterial design by using spiral resonators," Phys. Rev. B: Condens. Matter **69**, art. no. 014402 (2004).
16. E. Lenz and H. Henke, "Homogenization of metamaterials due to fractaloid structures in the microwave regime," J. Opt. A: Pure Appl. Opt. **11**, art. no. 114021 (2009).
17. H. Chen, L. Ran, B.-I. Wu, J. A. Kong, and T. M. Grzegorczyk, "Crankled S-ring resonator with small electrical size," Progress in Electromagnetics Research **66**, 179–190 (2006).
18. D. Schurig, J. J. Mock, and D. R. Smith, "Electric-field-coupled resonators for negative permittivity metamaterials," Appl. Phys. Lett. **88**, art. no. 041109 (2006).
19. W. J. Padilla, M. T. Aronsson, C. Highstrete, M. Lee, A. J. Taylor, and R. D. Averitt, "Electrically resonant terahertz metamaterials: Theoretical and experimental investigations," Phys. Rev. B: Condens. Matter **75**, art. no. 041102 (2007).
20. K. C. Gupta, R. Garg, I. Bahl, and P. Bhartia, *Microstrip Lines and Slotlines* (Artech House, 1996), 2nd ed.
21. G. Houzet, X. Mélique, and D. Lippens, "Microstrip transmission line loaded by split-ring resonators tuned by ferroelectric thin film," Progress in Electromagnetics Research **12**, 225–236 (2010).
22. C. Caloz and T. Itoh, "Transmission line approach of left-handed (LH) materials and microstrip implementation of an artificial LH transmission line," IEEE Trans. Antennas Propag. **52**, 1159–1166 (2004).
23. A. Sanada, C. Caloz, and T. Itoh, "Characteristics of the composite right/left-handed transmission lines," IEEE Microwave Wireless Compon. Lett. **14**, 68–70 (2004).
24. I. J. Bahl, *Lumped Element for RF and Microwave Circuits* (Artech House, 2003).
25. G. D. Alley, "Interdigital capacitors and their application to lumped-element microwave integrated circuits," IEEE Trans. Microwave Theory Tech **MTT-18**, 1028–1033 (1970).
26. X. Chen, T. M. Grzegorczyk, B.-I. Wu, J. J. Pacheco, and J. A. Kong, "Robust method to retrieve the constitutive effective parameters of metamaterials," Phys. Rev. E **70**, art. no. 016608 (2004).
27. D. R. Smith, D. C. Vier, T. Koschny, and C. M. Soukoulis, "Electromagnetic parameter retrieval from inhomogeneous metamaterials," Phys. Rev. E **71**, art. no. 036617 (2005).
28. J. Zhang and Z. R. Hu, "A novel broadband metamaterial resonator with negative permittivity," in "PIERS Proceedings, Xi'an, China," (2010), pp. 1346–1348.
29. H. A. Wheeler, "Fundamental limits of small antennas," Proc. IRE. **35**, 1479–1484 (1947).
30. L. J. Chu, "Physical limitations of omni-directional antennas," J. Appl. Phys. **19**, 1163–1175 (1948).
31. R. F. Harrington, "Effect of antenna size on gain, bandwidth, and efficiency," J. Research National Bureau of Standards—D. Radio Propagation **64D** (1960).
32. M. A. Ordal, L. L. Long, R. J. Bell, S. E. Bell, R. R. Bell, J. R. W. Alexander, and C. A. Ward, "Optical properties of the metals Al, Co, Cu, Au, Fe, Pb, Ni, Pd, Pt, Ag, Ti, and W in the infrared and far infrared," Appl. Opt. **22**, 1099–1119 (1983).
33. J. Dai, J. Zhang, W. Zhang, and D. Grischkowsky, "Terahertz time-domain spectroscopy characterization of the far-infrared absorption and index of refraction of high-resistivity, float-zone silicon," J. Opt. Soc. Am. B **21**, 1379–1386 (2004).
34. K. Takano, T. Kawabata, C.-F. Hsieh, K. Akiyama, F. Miyamaru, Y. Abe, Y. Tokuda, R.-P. Pan, C.-L. Pan, and M. Hangyo, "Fabrication of terahertz planar metamaterials using asuper-fine ink-jet printer," Appl. Phys. Express, art. no. 016701 (2010).
35. W. Withayachumnankul and D. Abbott, "Metamaterials in the terahertz regime," IEEE Photonics J. **1**, 99–118 (2009).

## 1. Introduction

An electromagnetic metamaterial is a man-made composite material comprising a periodic array of subwavelength inclusions. Typically, a single metallic metamaterial inclusion can be considered as an *LC* resonant circuit with its inductance and capacitance influenced by its shape and dimensions. These resonators can collectively exhibit macroscopically observed effective values of permittivity and/or permeability that are not found in natural materials. Various forms of resonant inclusions have been introduced to date, e.g., a split-ring resonators (SRR) for a

#135576 - $15.00 USD Received 23 Sep 2010; revised 3 Nov 2010; accepted 23 Nov 2010; published 26 Nov 2010

magnetic response [1] or a pair of cut wires for negative refractive index [2]. Because of the possibility of engineering electromagnetic material properties, metamaterials offer immense opportunities in improving existing optical designs along with exploring unprecedented devices such as superlenses [3, 4] and invisibility cloaks [5, 6].

For these devices to function properly, the underlying metamaterials must be operated in the effective-medium regime, i.e., the lattice constant or unit cell size should be much smaller than $\lambda_0/4$, where $\lambda_0$ is the operating, i.e. resonant, wavelength [7]. Under this condition a collection of metamaterial elements appears nearly homogeneous to incident waves and can be characterized by an effective permittivity and permeability. As the unit cell size approaches $\lambda_0/4$, diffraction effects and poor refraction become significant [8]. These parasitic effects are detrimental to the performance of metamaterials in quasi-optical applications. For example, a large unit cell size imposes a limitation on the subwavelength resolution of a metamaterial superlens [9]. When the cell size is comparable to or larger than a quarter-wavelength, the effective material parameters lose their relevance [10]. There are however limits to size reduction, because simply shrinking the volume or area of metamaterial inclusions reduces the capacitance and inductance and hence disturbs other important characteristics of metamaterials. In order to preserve these characteristics, the inductance and capacitance per unit area must be increased accordingly.

In this paper, a practical approach to reducing the electrical footprint of ELC resonators is presented. Section 2 reviews some existing solutions to reduce the size of metamaterial resonators. Section 3 describes the design of IDC-loaded ELC resonators, along with a mathematical analysis based on lumped element theory. In Section 4, simulation and experimental results obtained from the proposed resonators are discussed in terms of the transmission characteristics and the effective medium properties.

## 2. Existing solutions

Several approaches can be implemented to increase the ratio between the operating wavelength and the unit cell size, i.e. the effective medium ratio, for various types of metamaterial resonators. In common, these approaches are based on the idea of raising the overall inductance and capacitance, which are related to the resonance frequency through $f_0 = 1/(2\pi\sqrt{LC})$. A straightforward way is to change the feature sizes of the structure, i.e., shorten gaps or lengthen wires to increase the capacitance and inductance, respectively. However, the realization of this simple approach can be limited by fabrication tolerances. As an alternative, increasing the permittivity or permeability of the host dielectric leads to a larger effective capacitance or inductance [8]. Despite a substantial reduction in the resonance frequency, the availability of the host medium with a high permittivity or permeability and low loss is an important issue. Furthermore, at some point the effective permeability can no longer be increased, irrespective of the intrinsic permeability of the substrate [11]. By integrating a surface-mounted capacitor onto a resonator, its resonance frequency can be tuned down significantly [12, 13]. However, loading the structure with lumped capacitive elements complicates the fabrication process and is not directly applicable to terahertz metamaterials.

A more sophisticated and specific approach involves redesigning the resonator pattern to accommodate a higher capacitance or inductance. As for example, a multiple SRR (MSRR) is an extension to a conventional SRR, within which smaller split rings are nested to increase the parallel capacitance [14]. With comparable dimensions, a spiral resonator (SR) has a larger capacitance than does a typical SRR by at least fourfold [15]. Essentially, an increment in the structural capacitance results in a realizable unit cell size down to $\lambda_0/40$ for an MSRR and $\lambda_0/250$ for an SR [14]. Fractal-based metamaterials with magnetic-field coupling similar to double SRR's have been reported [16]. The increased perimeter of the structure as a result

#135576 - $15.00 USD Received 23 Sep 2010; revised 3 Nov 2010; accepted 23 Nov 2010; published 26 Nov 2010

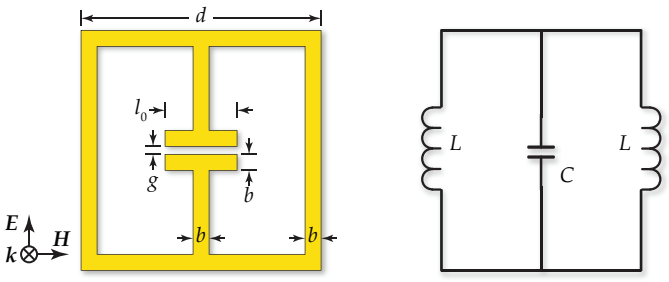


(a) ELC0 (b) equivalent circuit

Fig. 1. Electric-*LC* resonator. (a) A typical ELC resonator is composed of a center capacitive gap connected to two inductive loops. (b) An equivalent circuit of the resonator constitutes an *LC* resonator (the resistance is neglected here) [18].

of the fractal self-similarity leads to larger inductance and capacitance and a reduction in the resonance frequency. S-ring resonators that provide a double-negative response can be shrunken from $\lambda_0/6$ to $\lambda_0/15$ by winding parallel strips to increase the capacitance [17]. It is interesting to note that all the redesigned structures do not provide a pure electric resonance.

## 3. IDC-loaded ELC resonators

As a counterpart of the conventional magnetic SRR, an ELC resonator as shown in Fig. 1(a) provides a pure electric resonance with neither magnetic nor magnetoelectric responses, since the collective magnetic flux is nullified by virtue of the resonator's mirror symmetry [18, 19]. In the quasistatic limit, where the resonator size is much smaller than its operating wavelength, an ELC resonator can be approximated by the inductance and capacitance in the form of an *LC* resonance circuit, as illustrated in Fig. 1(b). During operation, an incident electric field with polarization perpendicular to the gap excites the capacitor to yield an electric resonance at $f_0 = 1/(\pi\sqrt{2LC})$. It was suggested that the resonance frequency of an ELC resonator can be tuned down by introducing more loops, or equivalently more inductance, to both arms [18]. However, the method requires additional fabrication steps, as the suggested structure is multilayered. Furthermore, such a design is incompatible with standard lithographic techniques, which are widely utilized for fabricating terahertz metamaterials. Other general approaches reviewed in the previous section might be adopted, with their respective limitations, to reduce the electrical size of the resonator.

A practical redesign of the structure presented in this article involves replacing the normal capacitive gap in the center of an ELC resonator with an interdigital capacitor (IDC), illustrated in Fig. 2, to increase the capacitance. Essentially, IDC's are widely used as lumped elements

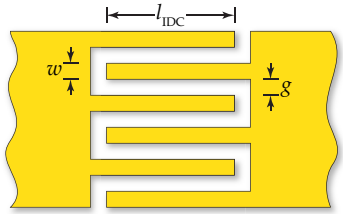


Fig. 2. Interdigital capacitor (IDC) with 6 fingers. The finger length $l_{IDC}$ extends over the overlapping portion of all fingers.

#135576 - $15.00 USD Received 23 Sep 2010; revised 3 Nov 2010; accepted 23 Nov 2010; published 26 Nov 2010

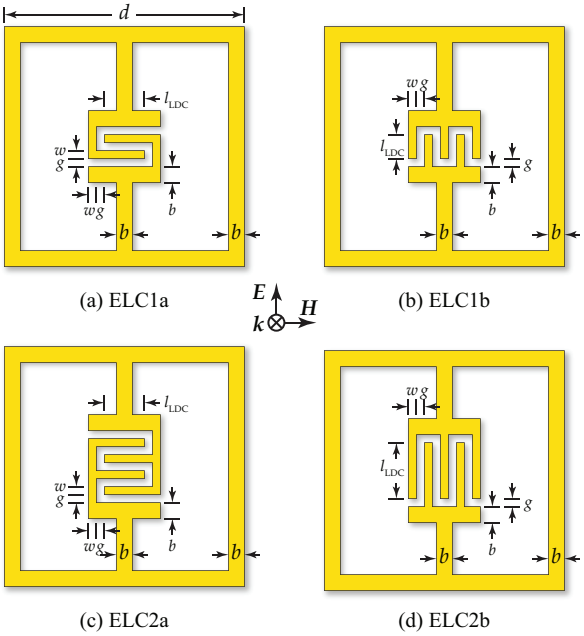


Fig. 3. Two variants of IDC-loaded ELC resonators. The IDC's gaps align (a,c) in perpendicular to and (b,d) in parallel with the direction of an incident electric field.

in microwave circuits [20] with an aim to decrease their circuit board footprint. As such, its concept well suits metamaterials, where the unit cell needs to be much smaller than the operating wavelength. The feature size of an IDC does not need to be finer than the gap width of an ordinary ELC resonator to enhance the capacitance. Fabrication of IDC's can be readily carried out with standard photolithographic techniques, since the structure is fully planar. The single-layered design of IDC-loaded ELC resonators eliminates additional fabrication steps that might be required in other approaches. Owing to this level of simplicity, this design is favorable for implementing electric metamaterials in the terahertz regime.

Earlier, IDC's are incorporated into microstrip-coupled tunable SRRs aimed at enhancing the local electric field strength at the capacitors' gaps [21]. The idea of using IDC's with metamaterials has also been realized in the transmission-line approach. Composite right/left handed transmission lines (CRLH-TL's), which exhibit a band of negative phase velocity, are typically fitted with a set of IDC's that act as series capacitors [22, 23]. Even though the effect of IDC's in transmission-line metamaterials are extensively investigated, no assumption can be made for IDC-loaded resonators because of the radical difference of the two approaches.

Two variants for IDC-loaded ELC resonators are proposed and studied in this article. For the first configuration shown in Fig. 3(a,c), the capacitor's gaps are oriented perpendicularly to the intended polarization of operation, and the two ports are positioned at the outermost fingers on both sides. Another configuration in Fig. 3(b,d) has the gaps oriented in parallel to the polarization. The ports are located at the terminal strips (the strips that join fingers together). For the first configuration, the local electric field inside the capacitive gap aligns with the electric polarization. Hence, this configuration is expected to perform better in terms of cell size reduction. It is worth noting that the mirror symmetry of the resonator is broken in the first configuration. However, this does not affect the cancellation of the magnetic dipoles, since the area of the two current loops of the resonator are still identical.

#135576 - $15.00 USD Received 23 Sep 2010; revised 3 Nov 2010; accepted 23 Nov 2010; published 26 Nov 2010

Analytically, the capacitance of the IDC shown in Fig. 2 is a function of the finger length $l_{\mathrm{IDC}}$, total number of fingers $N$, line width $w$, gap width $g$, and effective dielectric constant $\varepsilon_{\mathrm{re}}$, as indicated in the following formula [20, 24]:

$$C_{\mathrm{IDC}} = \frac{\varepsilon_{\mathrm{re}} 10^{-3}}{18\pi} \frac{K(k)}{K'(k)} (N-1) l_{\mathrm{IDC}} \quad (\mathrm{pF}) , \tag{1}$$

where the approximated ratio between the elliptic integrals of first kind $K(k)$ and its complement $K'(k)$ reads

$$\frac{K(k)}{K'(k)} = \begin{cases} \frac{1}{\pi} \ln\left[2\frac{1+\sqrt{k}}{1-\sqrt{k}}\right] & \text{for} \quad 0.707 \leq k \leq 1 \\ \frac{\pi}{\ln\left[2\frac{1+\sqrt{k'}}{1-\sqrt{k'}}\right]} & \text{for} \quad 0 \leq k < 0.707 , \end{cases} \tag{2}$$

and $k' = \sqrt{1-k^2}$; $k = \tan^2[0.25w\pi/(w+g)]$. All the lengths are in microns. An ordinary parallel-strip capacitor can be approximated as an IDC with $N = 2$, the capacitance of which can be deduced from Eq. (1) as

$$C_0 = \frac{\varepsilon_{\mathrm{re}} 10^{-3}}{18\pi} \frac{K(k)}{K'(k)} l_0 \quad (\mathrm{pF}) , \tag{3}$$

where $l_0$ is the strip length (see Fig. 1). Provided that an IDC and a parallel-strip capacitor possess the same line width, gap width, and substrate type, their capacitances can be related through

$$C_{\mathrm{IDC}} = (N-1) \frac{l_{\mathrm{IDC}}}{l_0} C_0 . \tag{4}$$

The factor $l_{\mathrm{IDC}}/l_0$ compensates the difference between the finger length and strip length.

For an ELC resonator, if the inductance loop remains unchanged, it can be estimated from Eq. (4) that the new resonance frequency $f_{0,\mathrm{new}}$ after IDC loading equals

$$f_{0,\mathrm{new}} = \sqrt{\frac{l_0}{l_{\mathrm{IDC}}(N-1)}} f_0 , \tag{5}$$

where $f_0$ is the resonance frequency of a conventional ELC resonator. This simple model gives an impression for the expected change in the resonance frequency of IDC-loaded ELC resonators.

## 4. Results

### *4.1. Transmission characteristics*

The four designs of IDC-loaded ELC resonators in Fig. 3, along with a corresponding conventional resonator in Fig. 1, are fabricated and characterized in the microwave regime. For the sake of comparison, the five designs share the unit cell size $a$, gap width $g$, and cross-sectional length of the loaded capacitor. It is suggested that the finger width should be equal to the gap width, or $w = g$, to maximize the capacitance density [25]. In details, the structural parameters common to all designs are $w = g = 0.4$ mm, $b = 0.8$ mm, $d = 12$ mm, and $a = 14$ mm. Other parameters specific to each design are given in Table 1. Each planar metamaterial comprises an array of 9×9 identical resonators, made of copper with a thickness of 35.6 $\mu$m (1.4 mil). The planar substrate is an FR4 epoxy board with a thickness of 0.8 mm, a measured dielectric

#135576 - $15.00 USD Received 23 Sep 2010; revised 3 Nov 2010; accepted 23 Nov 2010; published 26 Nov 2010

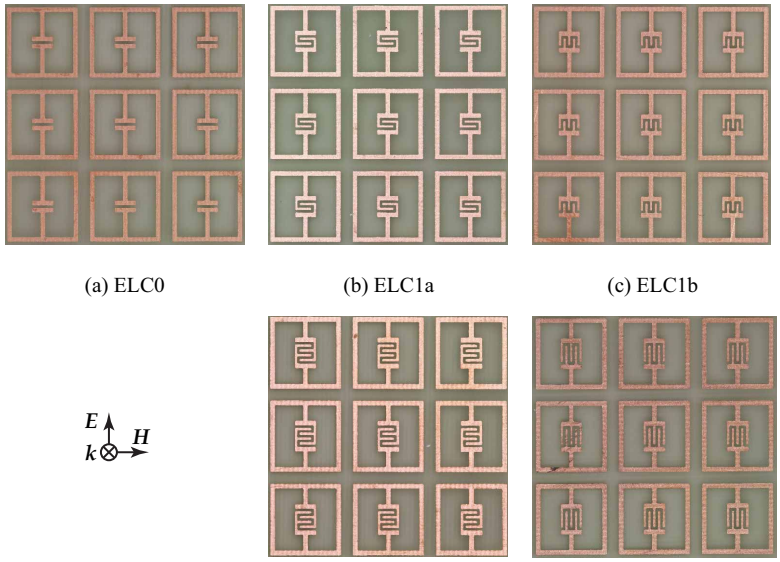


(a) ELC0 (b) ELC1a (c) ELC1b

(d) ELC2a (e) ELC2b

Fig. 4. ELC resonator arrays forming planar metamaterials used in the experiment. Each sample is fabricated from copper on an FR4 substrate. The photos show 3 by 3 arrays of resonators for convenience, however the actual array size used in the experiment was 9 by 9.

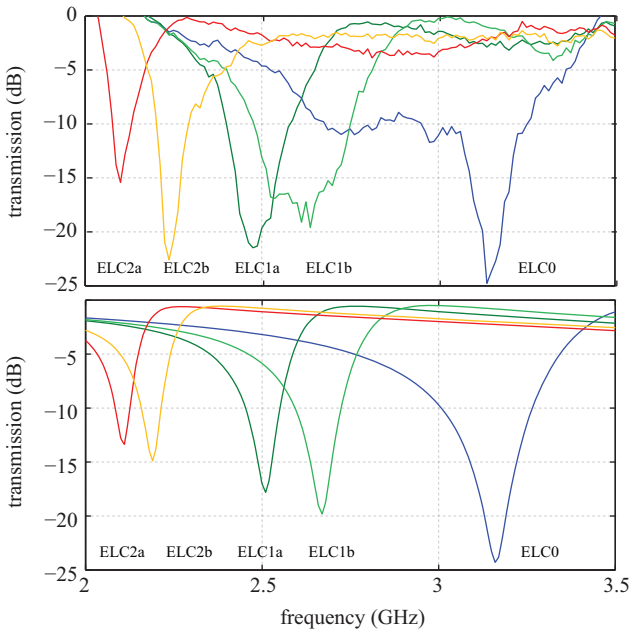


Fig. 5. Transmission profiles of the resonators from (top) the experiment and (bottom) the simulation. The two graphs share the horizontal scale.

#135576 - $15.00 USD Received 23 Sep 2010; revised 3 Nov 2010; accepted 23 Nov 2010; published 26 Nov 2010

constant of 4.2, and a reported loss tangent of 0.02. Partial views of the fabricated samples are shown in Fig. 4. In the experiment, a metamaterial sample is located between two horn antennas facing each other, from which the transmission through the sample is measured and compared to free-space transmission. The measurement results are given in Fig 5(top).

In order to verify the experimental results, the simulation for IDC-loaded ELC resonators is performed with a finite-element-based electromagnetic solver, Ansoft HFSS. Periodic boundary conditions are utilized for the transverse boundaries to replicate an infinite planar array of the resonators. Two ports at the open ends allows to determine the response of the sample to a plane wave incident normally to the array. As shown in Fig. 5 the simulation results are in general agreement with the experimental data. The discrepancies are attributed to the finite size of the fabricated array and the nonuniformity among the resonators due to fabrication tolerances. Table 1 indicates a general agreement in the resonance frequencies obtained from the simulation and the experiment. In addition, Eq. 5 can provide a rough estimation in the resonance frequency. Note that in a 3D configuration, the interaction between layers might shift the resonance slightly.

It is clear from Fig. 5 and Table 1 that the resonance frequency of IDC-loaded ELC resonators is remarkably lower than that of the original design. As a consequence, the coupling strength reduces for those structures with a higher capacitance [18, 13]. With a comparable capacitance area and density, sample ELC1a (ELC2a) has a lower resonance frequency compared to sample ELC1b (ELC2b). A reduction in resonance frequency is stronger when the gaps of the IDC are perpendicular to the polarization, as in ELC1a and ELC2a, which can be attributed to a better coupling between the incident electric field and the field in the capacitors. In terms of the effective medium ratio, the maximum improvement can be observed in sample ELC2a, for which $\lambda_0/a$ equals 10.2, in comparison to 6.8 of the conventional ELC design (ELC0). The effective medium ratio of other samples is listed in Table 1. Note that the original ELC design [18] has a unit cell size of $\lambda_0/5.7$.

### *4.2. Effective medium properties*

In order to provide further insight, the samples are characterized for their effective medium parameters. It is worth nothing that the parameters are evaluated on the basis of planar metamaterials. Hence, these parameters would need to be fine-tuned for 3D operation to take into account the weak inter-layer coupling. Here, the effective permittivity and permeability are extracted from the simulated transmission/reflection magnitude and phase using the method of Chen *et al.* [26]. For phase de-embedding, it is assumed that the thickness of a metamaterial sample in the direction of wave propagation is equal to the unit cell size or 14 mm in the present case [18]. Fig. 6 shows the effective permittivity and permeability of the selected resonators. It is obvious that the resonance frequency in the permittivity curve is lowered by the influence of

Table 1. The structural parameters and resonance frequency of the samples under test.

| Sample | $N$ | $l_{\mathrm{IDC}}$ (mm) | $f_0$ (GHz) | | | $\lambda_0/a$ |
|---|---|---|---|---|---|---|
| | | | simulated | estimated | measured | |
| ELC0 | 2 | $l_0 = 3.6$ | 3.16 | - | 3.14 | 6.8 |
| ELC1a | 4 | 2.0 | 2.51 | 2.45 | 2.48 | 8.7 |
| ELC1b | 5 | 1.2 | 2.67 | 2.74 | 2.64 | 8.1 |
| ELC2a | 6 | 2.0 | 2.11 | 1.90 | 2.10 | 10.2 |
| ELC2b | 5 | 2.8 | 2.19 | 1.79 | 2.24 | 9.6 |

#135576 - $15.00 USD Received 23 Sep 2010; revised 3 Nov 2010; accepted 23 Nov 2010; published 26 Nov 2010

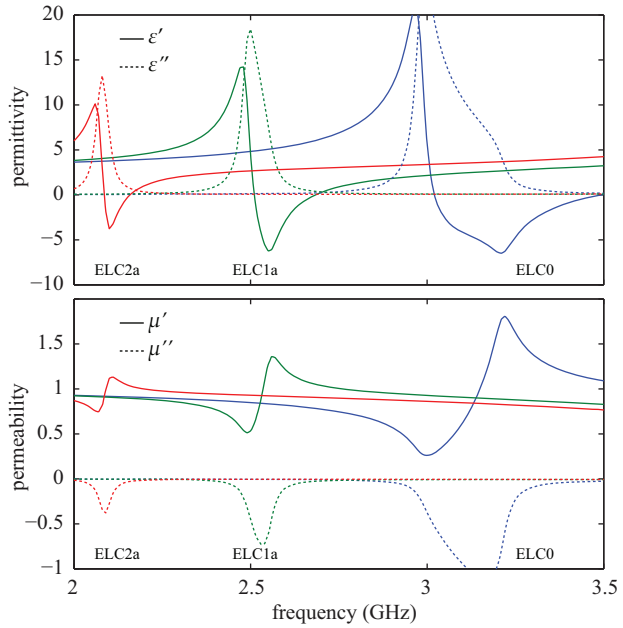


Fig. 6. The simulated effective medium properties of the samples; (top) the effective permittivity, and (bottom) the effective permeability. The two graphs share the horizontal scale.

IDC loading. The permittivity further illustrates a narrower bandwidth and a higher effective loss tangent in IDC-loaded ELC resonators. Despite that, the negative value of the permittivity is appropriate for typical applications requiring $\varepsilon = -1$. In addition, further simulation results (not shown here) indicate that with a lower-loss substrate, the effective loss tangent can be significantly reduced.

As discussed earlier, ELC resonators essentially possess no magnetic response, i.e., the real part of the permeability is close to unity over the frequencies of interest. However, the retrieved parameters do not strictly comply with this principle. As shown in Fig. 6, the real permeability becomes anti-resonant, and the imaginary part is negative. In fact, these anomalies are artifacts introduced during parameter extraction due to the inhomogeneity of metamaterials [7, 18, 27]. The reduction of these anomalies for ELC1a and ELC2a results from a lower dispersion and the higher homogeneity in these structures.

It is worth noting the characteristics of metamaterials from this and other designs [19, 28] suggest that there might exist a fundamental limit in the electrical size of the resonator in terms of the operating bandwidth. Such a limit could be in analogy to the well-known trade-off between the size and performance of an antenna [29, 30, 31], which operates on the basis of a resonance mechanism as well. Therefore, this potential trade-off for metamaterials deserves further theoretical investigation.

## 5. Conclusion

This article proposes to miniaturize ELC resonators through IDC loading. In the experiment, a set of IDC-loaded ELC samples is fabricated and characterized in the microwave frequency range. The measurement data, in agreement with the simulation results, reveal a significant improvement in the effective medium ratio of these IDC-loaded resonators. The parameter retrieval suggests a tradeoff between the electrical size and absorption in the proposed structure.

#135576 - $15.00 USD Received 23 Sep 2010; revised 3 Nov 2010; accepted 23 Nov 2010; published 26 Nov 2010

However, this issue can be partly alleviated by using a substrate with lower loss. An implication of metamaterial size reduction is the structural homogeneity, which leads to lower parasitic effects and hence a higher performance for quasi-optical applications.

The IDC-loading approach can be used in conjunction with other approaches to minimize the electrical size of ELC resonators. Apart from that, the proposed approach can be implemented when other options are not available due to fabrication limits. In addition, the IDC loading can be applied to other resonance-based metamaterials as well. Last but not least, the reduction of the resonator size is not only beneficial for metamaterial homogeneity but also useful in applications of metamaterial-based sensors, where a smaller electrical size of these structures is of a prime importance.

Owing to the scalability, the proposed structure is readily implementable in the terahertz frequency regime under the consideration of higher ohmic loss introduced by metal. In order to maximize the performance, it is suggested that a noble metal such as silver that has high conductivity in the terahertz regime [32] be a good choice. This will maximize coupling strength and minimize dissipation. A substrate such as high-resistivity silicon with negligible absorption [33] is also recommended to lessen the dissipation in the substrate. The form of the proposed structure is fully compatible with planar fabrication technologies, e.g., photolithography or super-fine inkjet printing [34], which are common to fabricating terahertz metamaterials [35].

**Acknowledgments**

The authors acknowledge Pavel Simcik for his technical assistance. This research was supported under the Australian Research Council *Discovery Projects* funding scheme (project number DP1095151).

#135576 - $15.00 USD Received 23 Sep 2010; revised 3 Nov 2010; accepted 23 Nov 2010; published 26 Nov 2010